

Karhunen-Loève Eigenvalue Problems in Cosmology: How should we Tackle Large Data Sets?

Max Tegmark^{1,2,4}, Andy N. Taylor³, & Alan F. Heavens³

¹*Institute for Advanced Study, Olden Lane, Princeton, NJ 08540*

²*Max-Planck-Institut für Astrophysik, Karl-Schwarzschild-Str. 1, D-85740 Garching*

³*Institute for Astronomy, University of Edinburgh, Royal Observatory, Blackford Hill, Edinburgh, U.K.*

⁴*Hubble Fellow*

max@ias.edu, ant@roe.ac.uk, afh@roe.ac.uk

26 November 2024

ABSTRACT

Since cosmology is no longer “the data-starved science”, the problem of how to best analyze large data sets has recently received considerable attention, and Karhunen-Loève eigenvalue methods have been applied to both galaxy redshift surveys and Cosmic Microwave Background (CMB) maps. We present a comprehensive discussion of methods for estimating cosmological parameters from large data sets, which includes the previously published techniques as special cases. We show that both the problem of estimating several parameters jointly and the problem of not knowing the parameters a priori can be readily solved by adding an extra singular value decomposition step.

It has recently been argued that the information content in a sky map from a next generation CMB satellite is sufficient to measure key cosmological parameters (h , Ω , Λ , *etc.*) to an accuracy of a few percent or better — in principle. In practice, the data set is so large that both a brute force likelihood analysis and a direct expansion in signal-to-noise eigenmodes will be computationally unfeasible. We argue that it is likely that a Karhunen-Loève approach can nonetheless measure the parameters with close to maximal accuracy, if preceded by an appropriate form of quadratic “pre-compression”.

We also discuss practical issues regarding parameter estimation from present and future galaxy redshift surveys, and illustrate this with a generalized eigenmode analysis of the IRAS 1.2 Jy survey optimized for measuring $\beta \equiv \Omega^{0.6}/b$ using redshift space distortions.

Key words: Cosmology: theory, large scale structure of Universe, cosmic microwave background – Astronomical methods: data analysis, statistical

1 INTRODUCTION

The problem of analysis of large data sets is one that, until recently, has not been a major concern of cosmologists. Indeed, in some areas no data existed to be analyzed. In the last few years, this situation has rapidly changed. A highlight in this transition has been the discovery of fluctuations in the cosmic microwave background (CMB) by the Cosmic Background Explorer (COBE) satellite (Smoot *et al.* 1992). In its short lifetime, COBE produced such a large data set that a number of sophisticated data-analysis methods were developed specifically to tackle it. In addition, the advent of large galaxy redshift surveys has created a field where the data sets increase by an order of magnitude in size in each generation. For instance, the surveys where

the object selection was based on the Infrared Astronomy Satellite (IRAS) contain several thousand galaxies: $\sim 2,000$ (QDOT; Lawrence *et al.* 1996) $\sim 5,000$ (Berkeley 1.2Jy; Fisher *et al.* 1995) and $\sim 15,000$ (PSC-z; Saunders *et al.* 1996). The proposed next-generation surveys will have much larger numbers of objects — around 250,000 in the Anglo-Australian Telescope 2 degree Field galaxy redshift survey (Taylor 1995) and $\sim 10^6$ for the Sloan Digital Sky Survey (Gunn & Weinberg 1995). Similarly plate measuring machines, such as the APM at Cambridge and SuperCOSMOS at the Royal Observatory, Edinburgh, can produce very large catalogues of objects, and numerical simulations of galaxy clustering are even now capable of producing so much data

that the analysis and storage of the information is in itself a challenge.

A standard technique for estimating parameters from data is the brute force maximum likelihood method, which illustrates why people have been driven towards developing more sophisticated methods. For n data items (*e.g.*, pixels in a CMB map, or Fourier amplitudes from a transformed galaxy distribution), the maximum likelihood method requires inversion of an $n \times n$ matrix for each set of parameter values considered — and this is for the simplest possible case where the probability distribution is Gaussian. Since a next-generation CMB satellite might produce a high resolution sky map with $\sim 10^7$ pixels, and the CPU time required for an inversion scales as n^3 , a brute force likelihood analysis of this type of data set will hardly be feasible in the near future.

Fortunately, it is often possible to greatly accelerate a likelihood analysis by first performing some appropriate form of data compression, by which the data set is substantially reduced in size while nonetheless retaining virtually all the relevant cosmological information. In this spirit, a large number of data-compression methods have been applied in the analysis of both CMB maps (*e.g.* Seljak & Bertschinger 1993; Górski 1994) and galaxy redshift surveys (*e.g.* Davis & Peebles 1983; Feldman *et al.* 1994; Heavens & Taylor 1995). A powerful prescription for how to do this optimally is the Karhunen-Loève eigenvalue method (Karhunen 1947), which has recently been applied to both CMB maps (Bond 1994; Bunn 1995; Bunn & Sugiyama 1995) and redshift surveys (Vogeley 1995; Vogeley & Szalay 1996). The goal of this paper is to review the more general framework in which these treatments belong, and to present some important generalizations that will facilitate the analysis of the next generation of cosmological data sets.

The rest of this paper is organized as follows. In Section 2, we review some useful information-theoretical results that tell us how well parameters can be estimated, and how to determine whether a given analysis method is good or bad. In Section 3, we review the Karhunen-Loève data compression method and present some useful generalizations. In Section 4 we illustrate the theory with various cosmology applications, including the special case of the signal-to-noise eigenmode method. In Section 5 we discuss limitations of method and possible ways of extending it to make the analysis feasible for huge data sets such as a 10^7 pixel future CMB map. Finally, our results are summarized and discussed in Section 6.

2 HOW WELL CAN YOU DO WITHOUT DATA COMPRESSION?

How accurately can we estimate model parameters from a given data set? This question was basically answered 60 years ago (Fisher 1935), and we will now summarize the results, which are both simple and useful.

2.1 The classical results

Suppose for definiteness that our data set consists on n real numbers x_1, x_2, \dots, x_n , which we arrange in an n -dimensional

vector \mathbf{x} . These numbers could for instance denote the measured temperatures in the n pixels of a CMB sky map, the counts-in-cells of a galaxy redshift survey, the first n coefficients of a Fourier-Bessel expansion of an observed galaxy density field, or the number of gamma-ray bursts observed in n different flux bins. Before collecting the data, we think of \mathbf{x} as a random variable with some probability distribution $L(\mathbf{x}; \boldsymbol{\Theta})$, which depends in some known way on a vector of model parameters

$$\boldsymbol{\Theta} = (\theta_1, \theta_2, \dots, \theta_m). \quad (1)$$

Such model parameters might for instance be the spectral index of density fluctuations, the Hubble constant h , the cosmic density parameter Ω or the mean redshift of gamma-ray bursts. We will let $\boldsymbol{\Theta}_0$ denote the true parameter values and let $\boldsymbol{\Theta}$ refer to our estimate of $\boldsymbol{\Theta}$. Since $\boldsymbol{\Theta}$ is some function of the data vector \mathbf{x} , it too is a random variable. For it to be a good estimate, we would of course like it to be unbiased, *i.e.*,

$$\langle \boldsymbol{\Theta} \rangle = \boldsymbol{\Theta}_0, \quad (2)$$

and give as small error bars as possible, *i.e.*, minimize the standard deviations

$$\Delta\theta_i \equiv \left(\langle \theta_i^2 \rangle - \langle \theta_i \rangle^2 \right)^{1/2} \quad (3)$$

In statistics jargon, we want the BUE θ_i , which stands for the “Best Unbiased Estimator”.

A key quantity in this context is the so-called *Fisher information matrix*, defined as

$$\mathbf{F}_{ij} \equiv \left\langle \frac{\partial^2 \mathcal{L}}{\partial \theta_i \partial \theta_j} \right\rangle, \quad (4)$$

where $\mathcal{L} \equiv -\ln L$. Another key quantity is the *maximum likelihood estimator*, or *ML-estimator* for brevity, defined as the parameter vector $\boldsymbol{\Theta}_{\text{ML}}$ that maximizes the likelihood function $L(\mathbf{x}; \boldsymbol{\Theta})$. (Above we thought of $L(\mathbf{x}; \boldsymbol{\Theta})$ as a probability distribution, a function of \mathbf{x} . However, when limiting ourselves to a given data set \mathbf{x} and thinking of $L(\mathbf{x}; \boldsymbol{\Theta})$ as a function of the parameters $\boldsymbol{\Theta}$, it is customarily called the *likelihood function*.)

Using this notation, a number of powerful theorems have been proven (see *e.g.* Kenney & Keeping 1951 and Kendall & Stuart 1969 for details):

- (i) For any unbiased estimator, $\Delta\theta_i \geq 1/\sqrt{\mathbf{F}_{ii}}$.
- (ii) If there is a BUE $\boldsymbol{\Theta}$, then it is the ML-estimator or a function thereof.
- (iii) The ML-estimator is asymptotically BUE.

The first of these theorems, known as the Cramér-Rao inequality, thus places a firm lower limit on the error bars that one can attain, regardless of which method one is using to estimate the parameters from the data. This is the minimum error bar attainable on θ_i if all the other parameters are known. If the other parameters are estimated from the data as well, the minimum standard deviation rises to $\Delta\theta_i \geq (\mathbf{F}^{-1})_{ii}^{1/2}$.

The second theorem shows that maximum-likelihood (ML) estimates have quite a special status: if there is a best method, then the ML-method is the one. Finally, the third result basically tells us that in the limit of a very large data set, the ML-estimate for all practical purposes is the best estimate, the one that for which the Cramér-Rao inequality

becomes an equality. It is these nice properties that have made ML-estimators so popular.

2.2 The Fisher information matrix

Although the proof of the Cramér-Rao inequality is rather lengthy, it is quite easy to acquire some intuition for why the Fisher information matrix has the form that it does. This is the purpose of the present section.

Let us Taylor expand \mathcal{L} around the ML-estimate Θ . By definition, all the first derivatives $\partial\mathcal{L}/\partial\theta_i$ will vanish at the ML-point, since the likelihood function has its maximum there, so the local behavior will be dominated by the quadratic terms. Since $L = \exp[-\mathcal{L}]$, we thus see that the likelihood function will be approximately Gaussian near the ML-point. If the error bars are quite small, L usually drops sharply before third order terms have become important, so that this Gaussian is a good approximation to L everywhere. Interpreting L as a Bayesian probability distribution in parameter space, the covariance matrix \mathbf{T} is thus given simply by the second derivatives at the ML-point, as the inverse of the Hessian matrix:

$$(\mathbf{T}^{-1})_{ij} \equiv \frac{\partial^2 \mathcal{L}}{\partial\theta_i \partial\theta_j}. \quad (5)$$

Note that the Fisher information matrix \mathbf{F} is simply the expectation value of this quantity at the point $\Theta = \Theta_0$ (which coincides with the ML-point on average if the ML-estimate is unbiased). It is basically a measure of how fast (on average) the likelihood function falls off around the ML-point, *i.e.*, a measure of the width and shape of the peak. From this discussion, it is also clear that we can use its inverse, \mathbf{F}^{-1} , as an estimate of the covariance matrix

$$\mathbf{T} \equiv \langle \Theta \Theta^t \rangle - \langle \Theta \rangle \langle \Theta^t \rangle \quad (6)$$

of our parameter estimates when we use the ML-method.

2.3 The Gaussian case

Let us now explicitly compute the Fisher information matrix for the case when the probability distribution is Gaussian, *i.e.*, where (dropping an irrelevant additive constant $n \ln[2\pi]$)

$$2\mathcal{L} = \ln \det \mathbf{C} + (\mathbf{x} - \boldsymbol{\mu}) \mathbf{C}^{-1} (\mathbf{x} - \boldsymbol{\mu})^t, \quad (7)$$

where in general both the mean vector $\boldsymbol{\mu}$ and the covariance matrix

$$\mathbf{C} = \langle (\mathbf{x} - \boldsymbol{\mu})(\mathbf{x} - \boldsymbol{\mu})^t \rangle \quad (8)$$

depend on the model parameters Θ . Although vastly simpler than the most general situation, the Gaussian case is nonetheless general enough to be applicable to a wide variety of problems in cosmology. Defining the data matrix

$$\mathbf{D} \equiv (\mathbf{x} - \boldsymbol{\mu})(\mathbf{x} - \boldsymbol{\mu})^t \quad (9)$$

and using the well-known matrix identity $\ln \det \mathbf{C} = \text{Tr} \ln \mathbf{C}$, we can re-write equation (7) as

$$2\mathcal{L} = \text{Tr} [\ln \mathbf{C} + \mathbf{C}^{-1} \mathbf{D}]. \quad (10)$$

We will use the standard comma notation for derivatives, where for instance

$$\mathbf{C}_{,i} \equiv \frac{\partial}{\partial\theta_i} \mathbf{C}. \quad (11)$$

Since \mathbf{C} is a symmetric matrix for all values of the parameters, it is easy to see that all the derivatives $\mathbf{C}_{,i}$, $\mathbf{C}_{,ij}$, *etc.*, will also be symmetric matrices. Using the matrix identities $(\mathbf{C}^{-1})_{,i} = -\mathbf{C}^{-1} \mathbf{C}_{,i} \mathbf{C}^{-1}$ and $(\ln \mathbf{C})_{,i} = \mathbf{C}^{-1} \mathbf{C}_{,i}$, we thus obtain

$$2\mathcal{L}_{,i} = \text{Tr} [\mathbf{C}^{-1} \mathbf{C}_{,i} - \mathbf{C}^{-1} \mathbf{C}_{,i} \mathbf{C}^{-1} \mathbf{D} + \mathbf{C}^{-1} \mathbf{D}_{,i}]. \quad (12)$$

When evaluating \mathbf{C} and $\boldsymbol{\mu}$ at the true parameter values, we have $\langle \mathbf{x} \rangle = \boldsymbol{\mu}$ and $\langle \mathbf{x} \mathbf{x}^t \rangle = \mathbf{C} + \boldsymbol{\mu} \boldsymbol{\mu}^t$, which gives

$$\begin{cases} \langle \mathbf{D} \rangle &= \mathbf{C}, \\ \langle \mathbf{D}_{,i} \rangle &= 0, \\ \langle \mathbf{D}_{,ij} \rangle &= \boldsymbol{\mu}_{,i} \boldsymbol{\mu}_{,j}^t + \boldsymbol{\mu}_{,j} \boldsymbol{\mu}_{,i}^t. \end{cases} \quad (13)$$

Using this and equation (12), we obtain $\langle \mathcal{L}_{,i} \rangle = 0$. In other words, the ML-estimate is correct on average in the sense that the average slope of the likelihood function is zero at the point corresponding to the true parameter values. Applying the chain rule to equation (12), we obtain

$$\begin{aligned} 2\mathcal{L}_{,ij} = \text{Tr} [& - \mathbf{C}^{-1} \mathbf{C}_{,i} \mathbf{C}^{-1} \mathbf{C}_{,j} + \mathbf{C}^{-1} \mathbf{C}_{,ij} \\ & + \mathbf{C}^{-1} (\mathbf{C}_{,i} \mathbf{C}^{-1} \mathbf{C}_{,j} + \mathbf{C}_{,j} \mathbf{C}^{-1} \mathbf{C}_{,i}) \mathbf{C}^{-1} \mathbf{D} \\ & - \mathbf{C}^{-1} (\mathbf{C}_{,i} \mathbf{C}^{-1} \mathbf{D}_{,j} + \mathbf{C}_{,j} \mathbf{C}^{-1} \mathbf{D}_{,i}) \\ & - \mathbf{C}^{-1} \mathbf{C}_{,ij} \mathbf{C}^{-1} \mathbf{D} + \mathbf{C}^{-1} \mathbf{D}_{,ij}]. \end{aligned} \quad (14)$$

Substituting this and equation (13) into equation (4) and using the trace identity $\text{Tr}[\mathbf{A}\mathbf{B}] = \text{Tr}[\mathbf{B}\mathbf{A}]$, many terms drop out and the Fisher information matrix reduces to simply

$$\mathbf{F}_{ij} = \langle \mathcal{L}_{,ij} \rangle = \frac{1}{2} \text{Tr} [\mathbf{A}_i \mathbf{A}_j + \mathbf{C}^{-1} \mathbf{M}_{ij}], \quad (15)$$

where we have defined the matrices $\mathbf{A}_i \equiv \mathbf{C}^{-1} \mathbf{C}_{,i} = (\ln \mathbf{C})_{,i}$ and $\mathbf{M}_{ij} \equiv \langle \mathbf{D}_{,ij} \rangle = \boldsymbol{\mu}_{,i} \boldsymbol{\mu}_{,j}^t + \boldsymbol{\mu}_{,j} \boldsymbol{\mu}_{,i}^t$. This old and well-known result is also derived by Bunn (1995) and Vogeley & Szalay (1996).

2.4 An example: parameter estimation with a future CMB experiment

Let us illustrate the above results with a simple example where $\boldsymbol{\mu} = 0$ and \mathbf{C} is diagonal. Suppose a next generation CMB satellite generates a high-resolution all-sky map of the CMB fluctuations. Let us for the moment ignore the complication of the galactic plane, and expand the temperature distribution in spherical harmonics $a_{\ell m}$. We define our data vector \mathbf{x} as the set of these coefficients from $\ell = 2$ up to some cutoff ℓ_{\max} , *i.e.*, $n = (\ell_{\max} + 1)^2 - 4$ and $x_i = a_i$, where we have combined ℓ and m into a single index $i = 1, 2, 3, \dots$ as $i = \ell^2 + \ell + m + 1$. With the standard assumption that the CMB fluctuations are isotropic, we have

$$\begin{cases} \boldsymbol{\mu} &= 0, \\ \mathbf{C}_{ij} &= \delta_{ij} \left[C_\ell + \frac{4\pi\sigma^2}{N} e^{\theta_b^2 \ell(\ell+1)} \right]. \end{cases} \quad (16)$$

Here C_ℓ denotes the angular power spectrum of the CMB, and the second term incorporates the effects of instrumental noise and beam smearing (Knox 1995, Tegmark & Efstathiou 1996). N is the number of pixels in the sky map, σ is the *r.m.s.* pixel noise,

$$\theta_b \equiv \text{FWHM} / \sqrt{8 \ln 2} \approx 0.425 \text{ FWHM}, \quad (17)$$

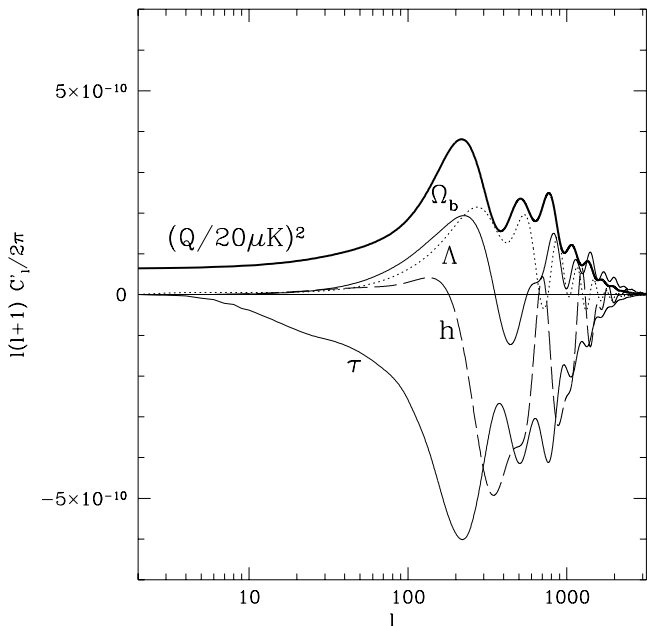


Figure 1. The derivatives of the CDM power spectrum with respect to various parameters.

and FWHM is the full-width-half-max beam width. Assuming that the CMB and noise fluctuations are Gaussian, equation (15) gives the Fisher information matrix

$$\mathbf{F}_{ij} = \sum_{\ell=2}^{\ell_{\max}} \left(\frac{2\ell+1}{2} \right) \left[C_{\ell} + \frac{4\pi\sigma^2}{N} e^{\theta_b^2 \ell(\ell+1)} \right]^{-2} \left(\frac{\partial C_{\ell}}{\partial \theta_i} \right) \left(\frac{\partial C_{\ell}}{\partial \theta_j} \right). \quad (18)$$

This handy expression, also derived by Jungman *et al.* (1996a), tells us that the crucial functions which determine the attainable accuracy are the *derivatives* of the power spectrum with respect to the various parameters. Examples of such derivatives are shown in Figure 1. For instance, the derivative with respect to the reionization optical depth, $\partial C_{\ell}/\partial \tau$, is shaped as $-C_{\ell}$ for $\ell \gg 10$, since earlier reionization suppresses all these multipoles by the same factor $e^{-2\tau}$. The derivative with respect to the quadrupole normalization, $\partial C_{\ell}/\partial Q$, of course has the same shape as the power spectrum itself.

Equation (18) has a simple geometric interpretation. We can think of the m functions $\partial C_{\ell}/\partial \theta_i$ as vectors in a Hilbert space of dimension $(\ell_{\max}-1)$, and think of the Fisher matrix component \mathbf{F}_{ij} as simply the dot product of the vectors $\partial C_{\ell}/\partial \theta_i$ and $\partial C_{\ell}/\partial \theta_j$. This dot product gives a rather small weight to low ℓ -values, essentially because there are fewer m -modes there and correspondingly larger cosmic variance. In addition, the weights are seen to be exponentially suppressed for large ℓ , where beam smearing causes the effect of pixel noise to explode. If the parameter dependence of C_{ℓ} was such that all n vectors $\partial C_{\ell}/\partial \theta_i$ were orthogonal under this dot product, then \mathbf{F} and the parameter covariance matrix $\mathbf{T} = \mathbf{F}^{-1}$ would be diagonal, and the errors in the estimates of the different parameters would be uncorrelated. The more similarly shaped two curves in Figure 1 are, the harder it will be to break the degeneracy between the corresponding two parameters. In the extreme case where two curves have

identical shape (are proportional to each other), the Fisher matrix becomes singular and the resulting error bars on the two parameters become infinite. It is therefore interesting to diagonalize the matrix \mathbf{T} (or equivalently, its inverse \mathbf{F}). The eigenvectors will tell us which m parameter combinations can be independently estimated from the CMB data, and the corresponding eigenvalues tell us how accurately this can be done.

It has been pointed out (Bond *et al.* 1994) that there will be a considerable parameter degeneracy if data is only available up to around the first Doppler peak. This is clearly illustrated in Figure 1: most of the curves lack strong features in this range, so some of them can be well approximated by linear combinations of the others. If a CMB experiment has high enough resolution to measure the power out to $l \sim 10^3$, however, this degeneracy is broken. Jungman *et al.* (1996b) compute the Fisher matrix for a model with the eleven unknown parameters

$$\Theta = (\Omega, \Omega_b, h^2, h, \Lambda, n_s, \alpha, n_T, T/S, \tau, Q, N_{\nu}); \quad (19)$$

the density parameter, the baryon density, the Hubble parameter, the cosmological constant, the spectral index of scalar fluctuations, the “running” of this index (a measure of the deviation from power law behavior), the spectral index of tensor fluctuations, the quadrupole tensor-to-scalar ratio, the optical depth due to reionization, and the number of light neutrino species, respectively. They find that even when estimating all these parameters simultaneously, the resulting error bars on some of the key parameters are of the order of a few percent or better for experiments with a resolution good enough to probe the first few Doppler peaks. Even the abundance of hot dark matter can be constrained in this fashion (Dodelson *et al.* 1996). An up-to-date discussion of which additional parameters can be constrained when using large-scale-structure data as well is given by Liddle *et al.* (1996).

It should be stressed that the formalism above only tells us what the attainable accuracy is if the truth is somewhere near the point in parameter space at which we compute the power derivatives. Figure 1 corresponds to standard COBE-normalized CDM, *i.e.*, to

$$\Theta_0 = (1, 0.015, 0.5, 0, 1, 0, 0, 0, 0, 20\mu\text{K}, 3). \quad (20)$$

The worst scenario imaginable would probably be extremely early reionization, since $\tau \gg 1$ would eliminate almost all small-scale power and introduce a severe degeneracy by making all the power derivatives almost indistinguishable for $\ell \gg 10$, the region where they differ the most in Figure 1.

Needless to say, accurate parameter estimation also requires that we can compute the theoretical power spectrum accurately. It has been argued (Hu *et al.* 1995) that this can be done to better than 1%, by accurately modeling various weak physical effects such as Helium recombination and polarization. We will return to other real-world issues, such as foreground contamination and incomplete sky coverage, further on.

3 OPTIMAL DATA COMPRESSION: KARHUNEN-LOËVE METHODS

Above we saw how small error bars one could obtain when using all the information in the data set. We also saw that for large data sets, these minimal error bars could be approximately attained by making a likelihood analysis using the entire data set. However, there are of course many situations where this approach is not feasible even in the simple Gaussian case.

3.1 The need for data compression

If we wish to estimate m parameters from n data points, this would involve inverting an $n \times n$ matrix at a dense grid of points in the m -dimensional parameter space. The CPU time required to invert such a non-sparse matrix scales as n^3 , and the number of grid points grows exponentially with m , so there are obviously limits as to what can be done in practice.

For instance, the “brute force” COBE analysis of Tegmark & Bunn (1995) had $n = 4038$ and $m = 2$, and involved inverting 4038×4038 matrices at a couple of hundred grid points. A future high-resolution all-sky CMB map might contain of order $n = 10^7$ pixels, and direct numerical inversion of matrices this large is clearly unfeasible at the present time. Also, to numerically map out the likelihood function in the 11-dimensional parameter space explored by Jungman *et al.* (1996b) with reasonable resolution would entail evaluating it at such a large number of grid points, that it would be desirable to make the inversion at each grid point as fast as possible.

Likewise, the spherical harmonic analysis of the 1.2Jy redshift survey (Heavens & Taylor, 1995, Ballinger Heavens & Taylor 1996), and the PSC-z survey (Tadros *et al.*, in preparation), required a likelihood analysis of some 1208 modes to find the redshift distortion parameter and a non-parametric stepwise estimate of the power spectrum.

Because of this, it is common to carry out some form of *data compression* whereby the n data points are reduced to some smaller set of n' numbers before the likelihood analysis is done. Since the time needed for a matrix inversion scales as n^3 , even a modest compression factor such as $n/n' = 5$ can accelerate the parameter estimation by more than a factor of 100.

3.2 The optimization problem

In this section, we will discuss the special case of *linear* data compression, which has as an important special case the so-called signal-to-noise eigenmode method. We will return to non-linear data compression methods below, in Section 5.

The most general linear data compression can clearly be written as

$$\mathbf{y} = \mathbf{B}\mathbf{x}, \quad (21)$$

where the n' -dimensional vector \mathbf{y} is the new compressed data set and \mathbf{B} is some arbitrary $n' \times n$ matrix. Thus the new data set has

$$\begin{cases} \langle \mathbf{y} \rangle & = \mathbf{B}\boldsymbol{\mu}, \\ \langle \mathbf{y}\mathbf{y}^t \rangle - \langle \mathbf{y} \rangle \langle \mathbf{y} \rangle^t & = \mathbf{B}\mathbf{C}\mathbf{B}^t, \end{cases} \quad (22)$$

and substituting this into equation (15) we find that the new Fisher information matrix $\tilde{\mathbf{F}}$ is given by

$$\begin{aligned} \tilde{\mathbf{F}}_{ij} &= \frac{1}{2} \text{Tr}[(\mathbf{B}\mathbf{C}\mathbf{B}^t)^{-1}(\mathbf{B}\mathbf{C}_{,i}\mathbf{B}^t)(\mathbf{B}\mathbf{C}\mathbf{B}^t)^{-1}(\mathbf{B}\mathbf{C}_{,j}\mathbf{B}^t) \\ &+ (\mathbf{B}\mathbf{C}\mathbf{B}^t)^{-1}(\mathbf{B}\mathbf{M}_{ij}\mathbf{B}^t)]. \end{aligned} \quad (23)$$

If $n = n'$ and \mathbf{B} is invertible, then the \mathbf{B} -matrices cancel in this expression, leaving us with simply

$$\tilde{\mathbf{F}}_{ij} = \frac{1}{2} \text{Tr}[\mathbf{B}^{-t}(\mathbf{A}_i\mathbf{A}_j + \mathbf{C}^{-1}\mathbf{M}_{ij})\mathbf{B}^t] = \mathbf{F}_{ij}. \quad (24)$$

In other words, \mathbf{B} just makes a similarity transform of the matrix within the trace in equation (15), leaving the Fisher information matrix \mathbf{F} unchanged. This reflects the fact that when \mathbf{B} is invertible, no information is lost or gained, so that the error bars on a measured parameter are unchanged. For instance, replacing a galaxy-cut COBE map consisting of say 3600 pixels by its spherical harmonic coefficients up to $\ell = 59$ (there are 3600 such coefficients) would be an invertible transformation, thus making no difference whatsoever as to the attainable error bars. Likewise, expansion in galaxy-cut spherical harmonics gives exactly the same result as expansion in an orthonormal basis for the galaxy-cut spherical harmonics (as in Górski 1994), since the mapping from the non-orthonormal basis to the orthonormal basis is invertible. This result is obvious if we think in terms of information: if the mapping from \mathbf{x} to \mathbf{y} is invertible, then \mathbf{y} must clearly contain exactly the same information that \mathbf{x} does, since we can reconstruct \mathbf{x} by knowing \mathbf{y} .

Rather, the interesting question is what happens when $n' < n$ and \mathbf{B} is not invertible. Each row vector of \mathbf{B} specifies one of the numbers in the new data set (as some linear combination of the original data \mathbf{x}), and we wish to know which such row vectors capture the most information about the parameters $\boldsymbol{\Theta}$. If \mathbf{B} has merely a single row, then we can write $\mathbf{B} = \mathbf{b}^t$ for some vector \mathbf{b} , and the diagonal ($i = j$) part of equation (23) reduces to

$$\tilde{\mathbf{F}}_{ii} = \frac{1}{2} \left(\frac{\mathbf{b}^t\mathbf{C}_{,i}\mathbf{b}}{\mathbf{b}^t\mathbf{C}\mathbf{b}} \right)^2 + \frac{(\mathbf{b}^t\boldsymbol{\mu}_{,i})^2}{(\mathbf{b}^t\mathbf{C}\mathbf{b})}. \quad (25)$$

Let us now focus on the problem of estimating a single parameter θ_i when all other parameters are known — we will return to the multi-parameter case below, in Section 3.6. Since the error bar $\Delta\theta_i \approx \tilde{\mathbf{F}}_{ii}^{-1/2}$ in this case, we want to find the \mathbf{b} that maximizes the right-hand side of equation (25). Although this is a non-linear problem in general, there are two simple special cases which between them cover many of the situations that appear in cosmology applications:

- The case where the mean is known: $\boldsymbol{\mu}_{,i} = 0$
- The case where the covariance matrix is known: $\mathbf{C}_{,i} = 0$

Below we show first how these two cases can be solved separately, then how the most general case can be for all practical purposes solved by combining these two solutions.

3.3 When the mean is known

When $\boldsymbol{\mu}$ is independent of θ_i , the second term in equation (25) vanishes, and we simply wish to maximize the quantity

$$(2\tilde{\mathbf{F}}_{ii})^{1/2} = \frac{|\mathbf{b}^t\mathbf{C}_{,i}\mathbf{b}|}{\mathbf{b}^t\mathbf{C}\mathbf{b}}. \quad (26)$$

Since the mean $\boldsymbol{\mu}$ does not depend on the parameters (*i.e.*, it is known), let us for simplicity redefine our data by $\boldsymbol{x} \mapsto \boldsymbol{x} - \boldsymbol{\mu}$, so that $\langle \boldsymbol{x} \rangle = 0$. Note that whereas the denominator in equation (26) is positive (since \mathbf{C} is a covariance matrix and thus positive definite), the expression $\mathbf{b}^t \mathbf{C}_{,i} \mathbf{b}$ in the numerator might be negative, since $\mathbf{C}_{,i}$ is not necessarily positive definite. We therefore want to make $(\mathbf{b}^t \mathbf{C}_{,i} \mathbf{b})/(\mathbf{b}^t \mathbf{C} \mathbf{b})$ either as large as possible or as small as possible, depending on its sign. Regardless of the sign, we thus seek the \mathbf{b} for which this ratio takes an extremum, *i.e.*, we want the derivatives with respect to the components of \mathbf{b} to vanish. Since this ratio is clearly unchanged if we multiply \mathbf{b} by a constant, we can without loss of generality choose to normalize \mathbf{b} so that the denominator equals unity. We thus seek an extremum of $\mathbf{b}^t \mathbf{C}_{,i} \mathbf{b}$ subject to the constraint that $\mathbf{b}^t \mathbf{C} \mathbf{b} = 1$.

$$(27)$$

This optimization problem is readily solved by introducing a Lagrange multiplier λ and extremizing the Lagrangean

$$\mathbf{b}^t \mathbf{C}_{,i} \mathbf{b} - \lambda \mathbf{b}^t \mathbf{C} \mathbf{b}. \quad (28)$$

Varying \mathbf{b} and setting the result equal to zero, we obtain the generalized eigenvalue problem

$$\mathbf{C}_{,i} \mathbf{b} = \lambda \mathbf{C} \mathbf{b}. \quad (29)$$

Since \mathbf{C} is symmetric and positive definite, we can Cholesky decompose it (*e.g.*, Press *et al.* 1992) as $\mathbf{C} = \mathbf{L} \mathbf{L}^t$ for some invertible matrix \mathbf{L} . Multiplying equation (29) by \mathbf{L}^{-1} from the left, we can rewrite it as

$$(\mathbf{L}^{-1} \mathbf{C}_{,i} \mathbf{L}^{-t})(\mathbf{L}^t \mathbf{b}) = \lambda (\mathbf{L}^t \mathbf{b}), \quad (30)$$

which we recognize as an ordinary eigenvalue problem for the symmetric matrix $(\mathbf{L}^{-1} \mathbf{C}_{,i} \mathbf{L}^{-t})$, whose solution will be n orthogonal eigenvectors $(\mathbf{L}^t \mathbf{b}_k)$ and corresponding eigenvalues λ_k , $k = 1, 2, \dots, n$. Let us sort them so that

$$|\lambda_1| \geq |\lambda_2| \geq \dots \geq |\lambda_n|. \quad (31)$$

Let us choose the k^{th} row of \mathbf{B} to be the row vector \mathbf{b}_k^t , so that the compressed data set is given by $y_k = \mathbf{b}_k^t \boldsymbol{x}$. The orthogonality property $(\mathbf{L}^t \mathbf{b}_k) \cdot (\mathbf{L}^t \mathbf{b}_{k'}) \propto \delta_{kk'}$ in combination with our chosen normalization of equation (27) then tells us that our compressed data satisfies

$$\langle y_k y_{k'} \rangle = \langle (\mathbf{b}_k^t \boldsymbol{x})(\boldsymbol{x}^t \mathbf{b}_{k'}) \rangle = \mathbf{b}_k^t \mathbf{C} \mathbf{b}_{k'} = \mathbf{b}_k^t \mathbf{L} \mathbf{L}^t \mathbf{b}_{k'} = \delta_{kk'}, \quad (32)$$

i.e., $\langle \mathbf{y} \mathbf{y}^t \rangle = \mathbf{I}$. The compressed data values \mathbf{y} thus have the nice property that they are what is known as *statistically orthonormal*, *i.e.*, they are all uncorrelated and all have unit variance. Since we are assuming that everything is Gaussian, this also implies that they are statistically independent — in fact, \mathbf{y} is merely a vector of independent unit Gaussian random variables. In other words, knowledge of y_k gives us no information at all about the other y -values. This means that the entire information content of the initial data set \boldsymbol{x} has been portioned out in disjoint pieces in the new compressed data set, where y_1 contains the most information about θ_i , y_2 is the runner up (once the information content of y_1 has been removed, y_2 contains the most information about θ_i), and so on.

If we use all the n vectors \mathbf{b}_k as rows in \mathbf{B} , then \mathbf{B} will be invertible, and we clearly have not achieved any compression at all. However, once this matrix \mathbf{B} has been found, the compression prescription is obvious: if we want a compressed

data set of size $n' < n$, then we simply throw away all but the first n' rows of \mathbf{B} . It is straightforward to show (see *e.g.* Therrien 1992; Vogeley & Szalay 1996) that if we fix an integer n' and then attempt to minimize $\Delta\theta_i$, we will arrive at exactly the same \mathbf{B} as with our prescription above (or this \mathbf{B} multiplied by some invertible matrix, which as we saw will leave the information content unchanged).

How does the error bar $\Delta\theta_i$ depend on the choice of n' ? Equation (29) implies that

$$\mathbf{C}_{,i} \mathbf{B}^t = \mathbf{C} \mathbf{B}^t \boldsymbol{\Lambda}, \quad (33)$$

where $\Lambda_{ij} \equiv \delta_{ij} \lambda_i$, *i.e.*, a diagonal matrix containing all the eigenvalues. Since equation (32) implies that

$$\mathbf{B} \mathbf{C} \mathbf{B}^t = \mathbf{I}, \quad (34)$$

it follows from equation (33) that

$$\mathbf{B} \mathbf{C}_{,i} \mathbf{B}^t = \boldsymbol{\Lambda}. \quad (35)$$

Therefore the diagonal part of equation (23) reduces to simply

$$2\tilde{F}_{ii} = \text{Tr}\{[(\mathbf{B} \mathbf{C} \mathbf{B}^t)^{-1} (\mathbf{B} \mathbf{C}_{,i} \mathbf{B}^t)]^2\} = \text{Tr} \boldsymbol{\Lambda}^2 = \sum_{k=1}^{n'} \lambda_k^2. \quad (36)$$

It is thus convenient to plot λ_k^2 as a function of the mode number k , as we have done in Figure 2 for the specific case of measuring the redshift distortion parameter from the 1.2Jy redshift survey, to see at what k the information content starts petering out. Alternatively, one can plot $\Delta\theta_i$ as a function of n' as in Figure 3 and see when the curve flattens out, *i.e.*, when the computational cost of including more modes begins to yield diminishing returns. If one feels uncomfortable about choosing n' by “eyeballing”, one can obtain a more quantitative criterion by noting that using only a single mode \mathbf{b}_k would give $\Delta\theta_i = 1/|\lambda_k|$. Thus the quantity $\theta_i |\lambda_k|$ can be thought of as the signal-to-noise ratio for the k^{th} mode, and one can choose to keep only those modes where this ratio exceed unity (or some other constant such as 0.2).

3.4 When the covariance matrix is known

When \mathbf{C} is independent of θ_i , the first term in equation (25) vanishes, and we simply wish to maximize the quantity

$$\tilde{F}_{ii} = \frac{\mathbf{b}^t \mathbf{M}_{ii} \mathbf{b}}{\mathbf{b}^t \mathbf{C} \mathbf{b}}. \quad (37)$$

Introducing a Lagrange multiplier λ and proceeding exactly as in the previous section, this is equivalent to the eigenvalue problem

$$(\mathbf{L}^{-1} \mathbf{M}_{ii} \mathbf{L}^{-t})(\mathbf{L}^t \mathbf{b}) = \lambda (\mathbf{L}^t \mathbf{b}). \quad (38)$$

However, since the matrix $\mathbf{M}_{ii} = 2\boldsymbol{\mu}_{,i} \boldsymbol{\mu}_{,i}^t$ is merely of rank one, this problem is much simpler than that in the previous section. Since the left hand side is

$$2(\mathbf{L}^{-1} \boldsymbol{\mu}_{,i})(\boldsymbol{\mu}_{,i}^t \mathbf{b}) \propto (\mathbf{L}^{-1} \boldsymbol{\mu}_{,i}), \quad (39)$$

it points in the direction $(\mathbf{L}^{-1} \boldsymbol{\mu}_{,i})$ regardless what the vector \mathbf{b} is, so the only non-trivial eigenvector of $(\mathbf{L}^{-1} \mathbf{M}_{ii} \mathbf{L}^{-t})$ is

$$(\mathbf{L}^t \mathbf{b}_1) = (\mathbf{L}^{-1} \boldsymbol{\mu}_{,i}), \quad (40)$$

with a corresponding eigenvalue

$$\lambda_1 = 2|\mathbf{L}^{-1}\boldsymbol{\mu}_i|^2 = \text{Tr}[\mathbf{C}\mathbf{M}_{ii}]. \quad (41)$$

All other eigenvalues vanish. In other words, $\mathbf{b}_1 = \mathbf{C}^{-1}\boldsymbol{\mu}_i$, and the new compressed data set consists of just one single number,

$$y_1 = \boldsymbol{\mu}_i^t \mathbf{C}^{-1} \mathbf{x} \quad (42)$$

which contains just as much information about the parameter θ_i as the entire data set \mathbf{x} did. Another way to see this is to compute the Fisher information before and after the compression, and note that

$$\tilde{\mathbf{F}}_{ii} = \mathbf{F}_{ii} = \boldsymbol{\mu}_i^t \mathbf{C}^{-1} \boldsymbol{\mu}_i. \quad (43)$$

In other words, all the information about θ_i in \mathbf{x} has been distilled into the number y_1 . Thus the ML-estimate of θ_i is just some function of y_1 . For the special case where $\boldsymbol{\mu}$ depends linearly on the parameter, *i.e.*, $\boldsymbol{\mu} = \boldsymbol{\mu}_i \theta_i$ where $\boldsymbol{\mu}_i$ is a known constant vector, this function becomes trivial: the expectation value of equation (42) reduces to

$$\langle y_1 \rangle = (\boldsymbol{\mu}_i^t \mathbf{C}^{-1} \boldsymbol{\mu}_i) \theta_i, \quad (44)$$

which means that on average, up to a known constant $(\boldsymbol{\mu}_i^t \mathbf{C}^{-1} \boldsymbol{\mu}_i)$, the compressed data is just the desired parameter itself.

3.5 When neither is known — the general case

In the most general case, both $\boldsymbol{\mu}$ and \mathbf{C} depend on the parameters $\boldsymbol{\Theta}$. This happens for instance in the CMB case when the components of \mathbf{x} are chosen to be estimates of the power spectrum C_ℓ , as in Section 5 below.

Clearly, the more ways in which the probability distribution for \mathbf{x} depends on the parameters, the more accurately we can estimate them. In other words, when both $\boldsymbol{\mu}$ and \mathbf{C} depend on $\boldsymbol{\Theta}$, we expect to do even better than in the two cases discussed above. Finding the vectors \mathbf{b} that extremize equation (25) is quite a difficult numerical problem. Fortunately, this is completely unnecessary. Solving the eigenvalue problem in Section 3.3 gives us n'' compression vectors capturing the bulk of the cosmological information coming from the first term in equation (25). Section 3.4 gives us one additional vector $\boldsymbol{\mu}_i^t \mathbf{C}^{-1}$ that captures all the cosmological information coming from the second term. In other words, if we simply use all these $n'' + 1$ compression vectors together, we have for all practical purposes solved our problem. Since a direct numerical attack on equation (25) could never reduce these $n'' + 1$ vectors to fewer than n'' without widening the resulting error bars, the time savings in the ensuing likelihood analysis would at most be a completely negligible factor $[(n'' + 1)/n'']^3 \sim 1 + 3/n''$ compared the simple prescription we have given here.

3.6 Estimating several parameters at once

The Karhunen-Loève method described above was designed to condense the bulk of the information about a *single* parameter into as few numbers y_k as possible. Although this particular problem does occasionally arise, most cosmology applications are more complicated, involving models that contain more than one unknown parameter. The

previous applications of Karhunen-Loève methods to CMB maps (Bond 1994; Bunn & Sugiyama 1995; Bunn 1995) and galaxy surveys (Vogeley 1995; Vogeley & Szalay 1996), have involved taking a rather minimalistic approach to this issue, by optimizing the eigenmodes for one particular parameter (typically the overall normalization of the fluctuations) and assuming that these eigenmodes will capture most of the relevant information about the other parameters as well.

If we want to estimate several parameters from a data set simultaneously, then how should we best compress the data? As we saw in Section 2, the covariance matrix \mathbf{T} of our parameter estimates $\boldsymbol{\Theta}$ is approximately \mathbf{F}^{-1} , so for the multivariate case, we have

$$\Delta\theta_i = (\mathbf{F}^{-1})_{ii}^{1/2} \quad (45)$$

instead of $\Delta\theta_i = \mathbf{F}_{ii}^{-1/2}$. One approach to the problem would thus be trying to minimize the diagonal elements of \mathbf{F}^{-1} rather than, as above, trying to minimize the diagonal elements of \mathbf{F} . This is, however, quite a cumbersome optimization problem.

Fortunately, there is an alternative solution to the problem which is easy to implement in practice and in addition is easy to understand intuitively, in terms of information content. Suppose that we repeat the standard KL procedure described above m times, once for each parameter θ_i , and let n'_i denote the number of modes that we choose to use when estimating the i^{th} parameter. We then end up with m different compressed data sets, such that the n'_i numbers in the i^{th} set contain essentially all the information that there was about θ_i . This means that the union \mathbf{y} of all these compressed data sets, consisting of

$$n'' = \sum_{i=1}^m n'_i \quad (46)$$

numbers, retains basically all the information from \mathbf{x} that is relevant for our joint estimation of all the parameters. The problem is of course that there might be plenty of redundancy in \mathbf{y} . Indeed, if we typically compressed by say a factor $n/n'_i \sim 10$ and had 11 parameters as in the CMB model of Jungman *et al.* (1996b), then we would have achieved a counterproductive “anti-compression” with $n'' > n$.

How can we remove the unnecessary “pork” from \mathbf{y} ? The n'_i eigenvectors selected via the KL compression method span a certain subspace of the n -dimensional space in which the data vector \mathbf{x} lives, and we can think of the data compression step as simply projecting the vector \mathbf{x} onto this subspace. For each parameter θ_i , we found such a subspace, and the redundancy stems from the fact that many of these subspaces overlap with one another, or point in very similar directions. In order to compress efficiently and yet retain almost all the the information about all the parameters, we want to find a small set of vectors that span as much as possible of the union of all the subspaces. As described in detail in *e.g.* Press *et al.* (1992), this is readily accomplished by making a *Singular Value Decomposition* (SVD) and throwing away all vectors corresponding to very small singular values. Let us define $\mathbf{B}_i = \mathbf{B}\mathbf{A}$, where \mathbf{B} is the KL compression matrix optimized for estimating the i^{th} parameter. Here we multiply the row vectors by their corresponding eigenvalues so that better vectors will receive more weight in what follows. Combining all the row vectors of the trans-

posed compression matrices \mathbf{B}_i^t into a single matrix, SVD allows us to factor this matrix as

$$(\mathbf{B}_1^t \dots \mathbf{B}_m^t) = \mathbf{U} \mathbf{A} \mathbf{V}^t, \quad (47)$$

where $\mathbf{U}^t \mathbf{U} = \mathbf{I}$, $\mathbf{V}^t \mathbf{V} = \mathbf{I}$ and the matrix \mathbf{A} is diagonal. One customarily writes $\mathbf{A} = \text{diag}\{\lambda_i\}$, and refers to the diagonal elements λ_i as the *singular values*. These are basically a generalization of eigenvalues to non-square matrices. We define our final compression matrix as

$$\mathbf{B} \equiv \mathbf{U}^t. \quad (48)$$

The columns of \mathbf{U} with corresponding non-zero singular values λ_i form an orthonormal set of basis vectors that span the same space as all the initial compression vectors together. The column vectors of \mathbf{U} with vanishing singular values form an orthonormal basis for the null-space of $\mathbf{U} \mathbf{A} \mathbf{V}^t$, representing redundant information. Similarly, the vectors corresponding to singular values near zero capture information that is almost entirely redundant. By making a plot similar to Figure 2, showing λ_k as a function of k , one decides on the final number $n' < n''$ of row vectors in \mathbf{B} to keep. Once n' has been fixed, one can of course (if one prefers^{*}) make the n' numbers in the new compressed data set statistically orthogonal as before by Cholesky decomposing their covariance matrix $\mathbf{B} \mathbf{C} \mathbf{B}^t = \mathbf{L} \mathbf{L}^t$ and replacing $\mathbf{z} = \mathbf{B} \mathbf{x}$ by $\mathbf{L}^{-t} \mathbf{z}$. In summary, we have found that when we wish to estimate more than one parameter from the data, we can obtain a close to optimal data compression with the following steps:

- (i) Compute the KL eigenmodes that contain the bulk of the information about the first parameter.
- (ii) Repeat this procedure separately for all other parameters.
- (iii) Arrange all the resulting vectors, multiplied by their eigenvalues, as the rows of \mathbf{B} .
- (iv) Make an SVD of \mathbf{B} and throw away all rows corresponding to very small singular values.

3.7 The problem of not knowing the parameters a priori

The KL-approach has sometimes been criticized for not being model-independent, in the sense that one needs to make an a priori guess as to what the true parameter values Θ_0 are in order to be able to compute the compression matrix \mathbf{B} . Although there is no evidence that a bad guess as to Θ_0 biases the final results (see *e.g.* Bunn 1995 for a detailed discussion of these issues, including numerical examples), a poor guess of Θ_0 will of course lead to a data compression that is no longer optimal. In other words, one would expect to still get an unbiased answer, but perhaps with larger error bars than necessary.

In practice, this loss of efficiency is likely to be marginal. For instance, as a test, Bunn (1995) performed a KL-analysis of a COBE CMB map with $n \sim 1$ assuming a blatantly erroneous spectral index $n = 2$ to compute B ($n = 2$ is ruled out at about 3σ a posteriori), and compared this with

* The only merit of the statistical orthogonality is that it will make $\langle \mathbf{y} \mathbf{y}^t \rangle$ more close to diagonal near the fiducial parameter values Θ , which might conceivably speed up the matrix inversion if an iterative method is used.

the results obtained when assuming $n = 1$. The error bars where found to change only marginally.

If one nonetheless wishes to do something about this efficiency problem, it is fortunately quite easy in practice. The simplest approach is an iterative scheme, whereby the KL-analysis is carried out twice, using the ML-estimate of Θ from the first run as the fiducial “true” value in the second run. A more rigorous approach is to compute compression vectors \mathbf{b} for a number of different assumptions about Θ_0 that include the extreme corners of parameter space, and then combine all these vectors into a single compression matrix \mathbf{B} by singular-value decomposition exactly as described in the previous section.

4 COSMOLOGY APPLICATIONS

In this section, we illustrate the theoretical discussion above with a number of cosmology examples, and show how the recently published work on CMB maps and galaxy surveys fits into the general KL-scheme as special cases. We will see that the typical compression factor is about 10 in both an IRAS example and a COBE example.

4.1 A large-scale-structure example: redshift-space distortions

Here we apply a KL-analysis to the problem of redshift-space distortions in the 1.2Jy IRAS galaxy survey (Fisher *et al.* 1995). This problem has previously been analyzed in detail by Heavens & Taylor (1995, hereafter HT95) who used a spherical harmonic analysis. Here we repeat their analysis, but include a KL data-compression step to investigate how many modes are needed for an accurate determination of the redshift distortion parameter

$$\beta \equiv \frac{\Omega^{0.6}}{b}, \quad (49)$$

where b denotes the conventional linear bias factor, the ratio between the fluctuations in luminous matter and the total matter fluctuations. As was first shown by Kaiser (1987), the peculiar motions of galaxies induces a characteristic radial distortion in the apparent clustering pattern that depends only on this parameter β .

As the initial data vector \mathbf{x} , we use the coefficients obtained by expanding the observed galaxy distribution in combinations of spherical harmonics and spherical Bessel functions as described in HT95, with the known mean values subtracted off so that $\boldsymbol{\mu} = \langle \mathbf{x} \rangle = 0$. HT95 show that the covariance matrix is given by

$$\mathbf{C}_{\mu\nu} = \Lambda_{\mu\nu}^{\text{sn}} + \frac{1}{2} \sum_{\alpha} (\boldsymbol{\Phi}_{\alpha\mu} + \beta \mathbf{V}_{\alpha\mu}) (\boldsymbol{\Phi}_{\alpha\nu} + \beta \mathbf{V}_{\alpha\nu}) P(k_{\alpha}), \quad (50)$$

where the indices μ, ν and α run over the above-mentioned modes, and $P(k)$ is the power spectrum. The matrices $\boldsymbol{\Phi}$ and \mathbf{V} encapsulate the effects of finite survey volume convolution and redshift distortions, respectively. The matrix Λ^{sn} contains the shot-noise contribution. All three matrices are independent of β . For our illustrative example, we assume a parametrised form of the power spectrum suggested by Peacock & Dodds (1994), which means that β is the only

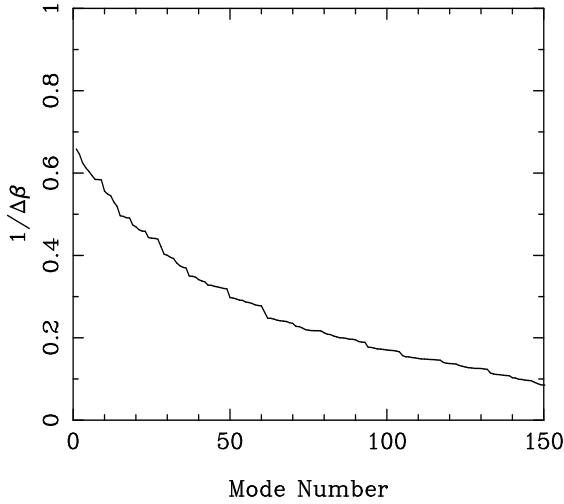


Figure 2. KL-eigenvalues $\lambda = 1/\Delta\beta$.

unknown parameter. Hence $m = 1$ and $\Theta = \theta_1 = \beta$. Differentiating equation (50), we obtain

$$\mathbf{C}_{,1} = \frac{\partial \mathbf{C}}{\partial \beta} = \frac{1}{2}(\mathbf{V}\mathbf{P}\Phi^t + \Phi\mathbf{P}\mathbf{V}^t) + (\mathbf{V}\mathbf{P}\mathbf{V}^t)\beta, \quad (51)$$

where $\mathbf{P}_{\alpha\beta} \equiv P(k_\alpha)\delta_{\alpha\beta}$ (i.e., $\mathbf{P} = \text{diag}\{P(k_\alpha)\}$). We assume an a priori value $\beta = 1$ to evaluate this matrix. Using $n = 1208$ modes in the initial data set \mathbf{x} as in HT95, we obtain the eigenvalues λ_k shown in Figure 2. The resulting error bar

$$\Delta\beta = \left[\sum_{k=1}^{n'} \lambda_k^2 \right]^{-1/2} \quad (52)$$

is plotted as a function of n' (the number of modes used) in Figure 3, and is seen to level out at around $n' = 100$. This means that although HT95 used $\sim 10^3$ modes to estimate β , almost all the information is actually contained in the best $\sim 10^2$ linear combinations of these modes. In other words, we can obtain basically identical results to those found in HT95 by using a compressed data set only 10% of the original size. Since the matrix inversion time scales as n'^3 , this compression factor of 10 thus allows the inversion to be carried out 1000 times faster.

4.2 A special case: the signal-to-noise eigenmode method

The above-mentioned example was rather generic in the sense that \mathbf{C} depended on Θ in a nonlinear way (in this case, \mathbf{C} depended quadratically on β). However, the special case of the KL-method where the parameter dependence is linear (or rather affine) is so common and important that it has acquired a special name: the *signal-to-noise eigenmode method*. This is the special case where $\mu = 0$, we have only one unknown parameter θ , and the covariance matrix can be written in the form

$$\mathbf{C} = \mathbf{S}\theta + \mathbf{N}, \quad (53)$$

where the known matrices \mathbf{S} and \mathbf{N} are independent of θ . For reasons that will become clear from the examples below,

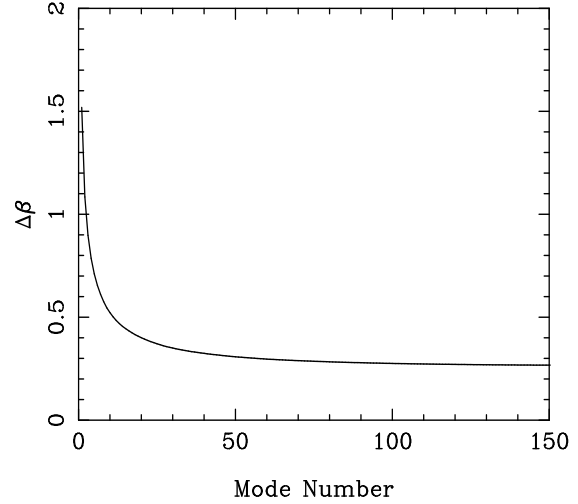


Figure 3. Error bar on beta β as a function of n' , the number of eigenmodes used.

\mathbf{S} and \mathbf{N} are normally referred to as the *signal* and *noise* matrices, respectively, and they are normally both positive definite. Since $d\mathbf{C}/d\theta = \mathbf{S}$, equation (29) gives the generalized eigenvalue problem

$$\mathbf{S}\mathbf{b} = \lambda(\mathbf{S} + \mathbf{N})\mathbf{b}. \quad (54)$$

By Cholesky decomposing the noise matrix as $\mathbf{N} = \mathbf{L}\mathbf{L}^t$, this is readily rearranged into the ordinary eigenvalue problem

$$(\mathbf{L}^{-1}\mathbf{S}\mathbf{L}^{-t})(\mathbf{L}^t\mathbf{b}) = \lambda'(\mathbf{L}^t\mathbf{b}), \quad (55)$$

where $\lambda' \equiv \lambda/(1 - \lambda)$. Since the matrix to be diagonalized, $(\mathbf{L}^{-1}\mathbf{S}\mathbf{L}^{-t})$, is loosely speaking $(\mathbf{N}^{-1/2}\mathbf{S}\mathbf{N}^{-1/2})$, a type of signal-to-noise ratio, its eigenvectors \mathbf{b} are usually referred to as the *signal-to-noise eigenmodes*. Historically, this terminology probably arose because one was analyzing one-dimensional time series with white noise, where $\mathbf{N} \propto \mathbf{I}$, so that $(\mathbf{L}^{-1}\mathbf{S}\mathbf{L}^{-t}) = \mathbf{S}\mathbf{N}^{-1}$ was the signal-to-noise ratio even in the strict sense. Vogeley & Szalay (1996) refer to the change of variables $\mathbf{x} \mapsto \mathbf{L}^{-1}\mathbf{x}$ as *prewhitening*, since it transforms $\mathbf{S} + \mathbf{N}$ into $(\mathbf{L}^{-1}\mathbf{S}\mathbf{L}^{-t}) + \mathbf{I}$, i.e., transforms the noise matrix into the white noise matrix, the identity matrix.

Equation (32) showed that in the general KL-case, the compressed data set was statistically orthonormal, $\langle \mathbf{y}\mathbf{y}^t \rangle = \mathbf{I}$. In the S/N-case, the compressed data has an additional useful property: both the signal and noise contributions to \mathbf{y} are uncorrelated *separately*. It is easy to show that

$$\mathbf{b}_k^t \mathbf{S} \mathbf{b}_{k'} = \lambda' \mathbf{b}_k^t \mathbf{N} \mathbf{b}_{k'} \propto \delta_{kk'}, \quad (56)$$

which means that the covariance matrix $\langle \mathbf{y}\mathbf{y}^t \rangle$ will remain diagonal even if we have misestimated the true signal-to-noise ratio. In other words, if the sole purpose of our likelihood analysis is to estimate the overall normalization θ from equation (53), we only need to invert diagonal matrices.

The signal-to-noise method arises in a wide variety of contexts. For instance, it is a special case not only of the KL-method, but also of the power spectrum estimation method of Tegmark (1996), corresponding to the case where the width of the window functions is ignored.

4.2.1 Signal-to-noise analysis of CMB maps

The signal-to-noise eigenmode method was introduced into CMB analysis by Bond (1994), who applied it to sky maps from both the COBE and FIRS experiments. It has also been applied to the COBE data by Bunn[†], and used it to constrain a wide variety of cosmological models (Bunn 1995; Bunn & Sugiyama 1995; Bunn, Scott & White 1995; Hu, Bunn & Sugiyama 1995; White & Bunn 1995; Yamamoto & Bunn 1996). Here the uncompressed data set consists of the CMB temperatures in n pixels from a sky map (for instance, $n = 4038$ or 4016 for a COBE map with a 20° galactic cut, depending on the pixelization scheme used). If foreground contamination is negligible (see *e.g.* Tegmark & Efstathiou 1996 for a recent review) and the pixel noise is uncorrelated (as it is for COBE to an excellent approximation — see Lineweaver *et al.* 1994) one has

$$\begin{cases} \mu &= 0, \\ \mathbf{S}_{ij} &= \sum_{\ell=2}^{\infty} \left(\frac{2\ell+1}{4\pi}\right) P_{\ell}(\hat{\mathbf{n}}_i \cdot \hat{\mathbf{n}}_j) W_{\ell}^2 C_{\ell}, \\ \mathbf{N}_{ij} &= \delta_{ij} \sigma_i^2, \end{cases} \quad (57)$$

where $\hat{\mathbf{n}}_i$ is a unit vector pointing the direction of the i^{th} pixel, σ_i is the *r.m.s.* noise in this pixel, P_{ℓ} are the Legendre polynomials and W_{ℓ} is the experimental beam function. This expression for \mathbf{S} should only be used if one marginalizes over the monopole and dipole in the ensuing likelihood analysis — otherwise \mathbf{S} should be corrected as described in Tegmark & Bunn (1995). In all the above-mentioned applications, the compression was optimized with respect to the overall normalization of the power spectrum (say $\theta = C_2$), so the matrix \mathbf{S} was independent of θ . It has been found (Bunn & Sugiyama 1995) that a compression factor of about 10, down to $n' \sim 400$ modes, can be attained without significant loss of information. This is about the same compression factor that we obtained in our redshift distortion example above.

Although these above-mentioned papers constrained a wide variety of cosmological parameters, the compression was in all cases optimized only for one parameter, the overall power spectrum normalization. Although this procedure can be improved as was described in Section 3.6, this does not appear to be causing substantial loss of efficiency in the COBE case. Support for this conclusion is provided by Tegmark & Bunn (1995), where it is found that KL-compression optimized for measuring the normalization gives error bars on the spectral index n that are less than 10% away from the minimal value that is obtained without any compression at all. It should also be noted that if one optimized the KL-compression for a different parameter θ , say $\theta = n$, then \mathbf{C} would no longer be of the simple form of equation (53). Thus the signal-to-noise eigenmode treatment no longer applies, and the more general equation (29) must be used instead.

As has been pointed out by Górski (1994), the rapid fall-off of the COBE window function W_{ℓ} implies that virtually all the cosmological information in the COBE maps is contained in the multipoles $\ell \leq 30$. When implementing the KL-compression in practice, it is useful to take advantage

of this fact by replacing the data set by the 957 spherical harmonic coefficients $a_{\ell m}$ for $2 \leq \ell \leq 30$, since this reduces the size of the matrix to be diagonalized by about a factor 4. This is an example of what we will call *pre-compression*, and we will return to this topic below, in Section 5.

4.2.2 Signal-to-noise analysis of galaxy surveys

The application of the signal-to-noise eigenmode method to galaxy surveys was pioneered by Vogeley (1995) and has since been further elaborated by Vogeley & Szalay (1996). Although these are both method papers, deferring actual parameter estimation to future work, the former explicitly evaluates the eigenmodes for the CfA survey and shows that there are about 10^3 modes with a signal-to-noise ratio exceeding unity.

In galaxy survey applications, the noise matrix \mathbf{N} contains the contribution from Poisson shot noise due to the finite number of galaxies per unit volume, rather than on detector noise as in the CMB case. With galaxies, the question of what to use as the initial data vector \mathbf{x} is not as simple as in the CMB case, since there is no obviously superior way to “pixelize” the observed density field. Vogeley & Szalay (1996) divide space into a large number of disjoint volumes (“cells”), and derive the resulting signal matrix \mathbf{S} in the approximation of ignoring redshift distortions. One alternative is using “fuzzy” cells as discussed by Tegmark (1995), for instance averages of the galaxy distribution where the weight functions are Gaussians centered at some grid of points.

Another alternative, which has the advantage of making it easier to include the effect of redshift distortions, is to use the coefficients from an expansion in spherical harmonics and spherical Bessel functions as was done by HT95, Ballinger *et al.* (1995; hereafter BHT95) and in Section 4.1 above. In BHT95 the real space power spectrum of density perturbations was left as a free function, to be evaluated in a stepwise fashion, along with the distortion parameter. In the case of only estimating the power, by fixing β to some constant value, the problem reduces to a signal-to-noise eigenmode problem, but with m free parameters — the power at m specified wavenumbers. Due to the mixing of wavenumbers by the Φ and \mathbf{V} matrices, these are generally not independent and so we must apply the SVD method to construct orthogonal eigenmodes. This application will be discussed elsewhere.

We conclude this section with a few additional comments on the above-mentioned “pixelization” issue. Compared to a CMB analysis, a galaxy survey analysis involves one more step, which is reducing the point data to the “initial” data vector \mathbf{x} . What is the relation between the first step (weighting galaxies) and the second step (weighting modes)? In Feldman, Kaiser & Peacock (1994) and Heavens & Taylor (1995), schemes for optimal weighting of galaxy data were presented. This weighting of the data (step 1) is prior to and complementary to the mode-weighting discussed in this paper (step 2). The data-weighting is designed to maximize the signal-to-noise of individual modes, and one might intuitively expect thus this to be a good mechanism for obtaining large eigenvalues λ_k . The techniques of the present paper can then subsequently be used to trim the data in an optimal way. The data-weighting scheme alone does not guarantee that we get the best answer possible.

[†] In fact, both Bond and Bunn independently reinvented the entire KL-method.

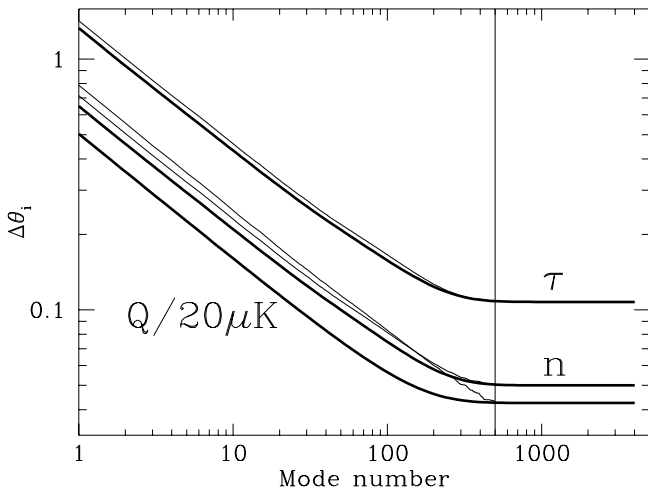


Figure 4. The three heavy lines show the smallest error bars attainable for the three parameters Q , n and τ as a function of the number of modes used, i.e., the error bars obtained when using the separately optimized KL-modes for each parameter. The three thin lines show the error bars obtained when using the 500 SVD modes, illustrating that these contain essentially all the relevant information about all three parameters.

This is because it maximizes the diagonal elements in the covariance matrix, ignoring correlations between modes. This does therefore not guarantee that the complete Fisher information matrix will be optimal. In general, it does not seem tractable to devise a data-weighting scheme which optimizes the Fisher matrix directly.

4.3 A multi-parameter CMB example

Here we apply a KL-analysis to the problem of estimating the quadrupole normalization Q , the spectral index n and the reionization optical depth τ from the 4-year COBE data (Bennett *et al.* 1996). As the initial data vector \mathbf{x} , we use the temperatures in the $N = 4016$ pixels that lie more than 20° from the galactic plane. Just as in Section 4.2.1, $\boldsymbol{\mu} = 0$ and $\mathbf{C} = \mathbf{S} + \mathbf{N}$ is given by equation (57). Computation of $\mathbf{C}_{,i}$ thus reduces to computing the derivatives of the angular power spectrum C_ℓ that occur in the sum, and we do this in practice using the software described in Seljak & Zaldarriaga (1996). The fiducial model has the standard CDM power spectrum shown in Figure 1. The three heavy lines in Figure 4 show the results of performing a separate KL-analysis for each parameter. In good agreement with the findings of Bunn & Sugiyama (1995), we see that virtually all information about Q is contained in the first 400 modes. Similarly, we see that all essentially all the information about n and τ is contained in the first 400 modes optimized for these parameters. Since the KL-modes for a parameter by construction give the smallest error bars, the curves corresponding to any other choice of modes would lie above these solid curves. For instance, if we used the KL-modes optimized for τ to measure Q , the resulting curve would lie above the bottom one if we were to plot it in Figure 4. Figure 1 provides a simple interpretation of this: since $dC_\ell/d\tau \approx 0$ for $\ell \ll 10$, the τ -modes do not contain information about the lowest multipoles, since this information

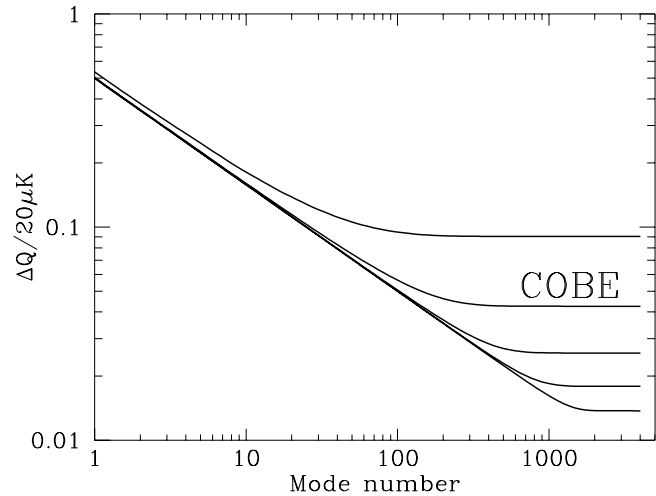


Figure 5. The error bars on the power spectrum normalization are shown for hypothetical COBE experiments with different noise levels. From top to bottom, they correspond to a noise enhancement factor 10, the real 4 year data, and noise reduction factors of 10, 100 and 1000.

is useless for measuring τ (even though it is important for measuring Q).

We implement the SVD technique described in Section 3.6 by taking the 500 best modes for each parameter and SVD-compressing these down to 500 modes. The thin lines in Figure 4 show the resulting error bars. We see that although they lie above the minimal curves for $k \ll 500$, they all “catch up” at $k = 500$. In other words, these 500 modes retain virtually all the relevant information about Q , n and τ , since using all of them gives virtually identical error bars to those obtained when using the full $N = 4016$ uncompressed data set.

4.4 A low noise CMB example

How effective will KL-compression be for future CMB data sets? Might it be the case that when noise levels are much lower, then all N KL-modes will have $S/N \gg 1$, so that no compression is possible? Figure 5 shows that the answer to the second question is no. For this example, we have repeated the above-mentioned COBE analysis for a range of different noise levels. With ten times less noise, the compression factor is seen to drop to about $4016/700 \sim 7$ and another order of magnitude of noise reduction lowers the compression factor to about 4. The upcoming MAP experiment forecasts a noise level $w^{-1} \equiv 4\pi\sigma^2/N \approx 2.5 \times 10^{-15}$, as compared to $w^{-1} \approx 10^{-12}$ for COBE and $w^{-1} \approx 5 \times 10^{-18}$ for the planned COBRAS/SAMBA experiment. These are quadratic quantities, so taking square roots, we see that MAP and COBRAS/SAMBA reduce the COBE noise by factors around 20 and 450, respectively. Figure 5 shows that even with 1000 times less noise, a compression factor of 2 is readily attainable. The explanation of this is oversampling. To avoid aliasing problems, the mean pixel separation must be smaller than the beam width by a substantial factor (the Shannon oversampling factor ~ 2.5). This redundancy remains even when the data set itself has excellent signal-to-

noise, so the KL-compression can take advantage of the fact that the pixel basis of the map is a sense overcomplete. Although future CMB experiments will of course have a much higher angular resolution than in our example, the oversampling factor will remain similar, so our conclusion about the usefulness of KL-compression will remain the same.

5 ON GIANT DATA SETS: THE NEED FOR PRE-COMPRESSSION

Above we have shown that the KL-compression technique is in many cases very useful. In this section, we will discuss some of its limitations, as well as outline nonlinear extensions that may make the compression technique feasible even for the next generation of CMB missions and galaxy surveys.

The number of pixels in a sky map from a next-generation CMB mission is likely to be around 10^7 . The Sloan Digital Sky Survey (SDSS) will measure the redshifts of 10^6 galaxies. Is it really feasible to apply KL-methods and likelihood analysis to data sets of this gargantuan size? We will argue that although an orthodox KL-analysis is *not* feasible, it appears as though the answer to the question may nonetheless be an encouraging yes if an extra nonlinear compression step is added to make the analysis doable in practice. Let us first note that despite the statistical orthogonality property of a KL-compressed data set, the matrices that need to be inverted to find the ML-estimate are in general *not* diagonal. BCB^t is only diagonal at the one point in parameter space where $\Theta = \Theta_0$, *i.e.*, the point corresponding to the parameter values that we assumed a priori. The ML-point generally lies elsewhere, and we need to find it by a numerical search in parameter space, so BCB^t will generally not even be sparse. This forces us to resort to Cholesky decomposition. For the $n \sim 4000$ case of Tegmark & Bunn (1995), this took about 10 minutes per matrix on a workstation. Since the time scales as n^3 and the storage as n^2 , this would require about 30 years of CPU time for $n = 10^6$, and about one terabyte of RAM. Even allowing for the exponential rate at which computer performance is improving, such a brute force likelihood analysis does not appear feasible for a megapixel CMB map within the next ten years.

The crucial question thus becomes how large a compression factor we can expect to achieve. We will argue that a factor of 10 is just about all one can do with linear compression, but that quadratic “pre-compression” may be able to gain another factor of 1000 for a next generation CMB experiment.

5.1 The limits of linear compression

Consider the following simple one-parameter example: we are given n numbers x_i drawn from a Gaussian distribution with zero mean and an unknown variance θ that we wish to estimate. Thus

$$\begin{cases} \boldsymbol{\mu} &= 0, \\ \boldsymbol{C} &= \theta I, \end{cases} \quad (58)$$

so when we solve equation (29), we find that all the eigenvalues are identical: $\lambda_k = 1/\theta$. Thus if we compress by keeping only the first n' modes, the resulting error bar will be

$$\Delta\theta = \sqrt{\frac{2}{n'}}\theta. \quad (59)$$

The fact that all eigenvalues are identical means that we would be quite stupid to throw away any modes at all, since they all contain the same amount of information. Simple as it is, this example nonetheless illustrates a difficulty with analyzing future CMB maps. Even in the best of all worlds, where we had complete sky coverage, we would encounter a problem of this type. To estimate a multipole C_ℓ , we would be faced with $(2\ell+1)$ coefficients $a_{\ell m}$ with zero mean and unknown variance, just as in the example above, which means that the KL-method would be of no use at all in compressing this data.

In Bunn (1995) and in one of the above examples, it was found that the COBE data set can be compressed down to about 400 numbers without losing much information. Where does this magic number 400 come from? In the absence of a galaxy cut, the number would probably be around 600, since beam smearing has eliminated virtually all information about multipoles $\ell \gtrsim 25$, and there are about 600 $a_{\ell m}$ -coefficients with $\ell < 25$. The fact that the galaxy cut removes about one third of the sky then reduces the cosmological information by about a third. There is also a more direct way to see where the compression factor 10 came from. As mentioned in Section 4.4, pixelized maps are generally oversampled by a factor 2.5 or more to avoid aliasing problems, which means that the mean pixel separation is considerable smaller than the beam width. Since the sky map is two-dimensional, the number of pixels per beam area is roughly the square of this number, of the order of 10. Future CMB missions will probably use similar oversampling rates, which means that a compression factor of 10 is probably the most we can hope for with linear compression only.

5.2 Quadratic compression

Fortunately, we are not limited to linear data compression. Let us compress the data set of our previous example into a single number defined by

$$y \equiv \frac{1}{n} \sum_{i=1}^n x_i^2. \quad (60)$$

Let us assume that n is very large, say $n \gtrsim 100$. Then y will be very close to Gaussian by the central limit theorem. This means that the mean is $\langle y \rangle = n\theta$ and the variance is $\langle y^2 \rangle - \langle y \rangle^2 = 2n\theta^2$. Substituting this into Equation (15) now gives

$$\Delta\theta = \sqrt{\frac{2}{n+4}}\theta \approx \sqrt{\frac{2}{n}}\theta, \quad (61)$$

i.e., the theoretically minimal error bar of equation (59) with $n' = n$. (The extra 4 in equation (61), which might seem to indicate that one can attain smaller error bars than the theoretical minimum, should of course be ignored — it merely reflects the fact that the Gaussian approximation breaks down for small n .)

In summary, we have found that whereas linear compression was powerless against our simple toy model, quadratic compression made mincemeat of the problem, condensing all the information into a single number. This result

is hardly surprising, considering that the compressed data set \mathbf{y} that we have defined in equation (60) is in fact the ML-estimate of the variance. It nonetheless has far-reaching implications for the issue of how to compress future CMB maps. If we have complete sky coverage, and define the compressed data set as

$$y_\ell \equiv \frac{1}{2\ell+1} \sum_{m=-\ell}^{\ell} |a_{\ell m}|^2, \quad (62)$$

then it is easy to show that the new Fisher information matrix will be identical to that of equation (18), which involved using the entire data set. For an experiment with a FWHM beamwidth of 4 arcminutes, there is virtually no information on multipoles above $\ell_{\max} = 3000$, so this means that in the absence of a galaxy cut, we could compress the entire data set into 3000 numbers without losing any cosmological information at all. Roughly speaking, this works because the compression throws away all the phase information and keeps all spherically averaged amplitude information, and it is the latter that contains all the information about the power spectrum. (For non-Gaussian models such as ones involving topological defects, the power spectrum alone does of course not contain all the relevant information.)

5.3 Real-world CMB maps: an outline of a compression recipe

The discussion above already included the effects of pixel noise and beam smearing. Barring systematic errors, there are two additional complications that will inevitably arise when analyzing future high-quality CMB maps:

- Foregrounds
- Incomplete sky coverage

Any attempts at foreground subtraction should of course be made before throwing away phase information, so that available spatial templates of galactic dust, radio point sources *etc.* can be utilized. For a recent discussion of such subtraction schemes, see *e.g.* Tegmark & Efstathiou (1996). The final result of the foreground treatment will almost certainly be a map where some regions, notably near the galactic plane, have been discarded altogether. The resulting incomplete sky coverage degrades information in two different ways:

- The sample variance increases.
- The spectral resolution decreases.

The former effect causes the variance in individual multipole estimates to grow as the inverse of the remaining sky area (Scott *et al.* 1994), and this increase in variance is automatically reflected in the final Fisher information matrix. The latter effect means that the y_ℓ defined by equation (62) is no longer a good estimate of the multipole C_ℓ . Rather, it is easy to show that $\langle y_\ell \rangle$ will be a weighted average of all the multipoles C_ℓ . These weights, known as the *window function*, generally form quite a broad distribution around ℓ , which means that the compressed data y_ℓ are effectively probing a smeared out version of the power spectrum. For a 20° galactic cut, this smearing is found to be around $\Delta\ell/\ell \sim 25\%$, which clearly destroys information about features such as the exact location of the Doppler peaks.

5.3.1 How to deal with incomplete sky coverage

Fortunately, the problem of incomplete sky coverage can be for all practical purposes eliminated. As described in detail by Tegmark (1996, hereafter T96), it is possible to obtain much narrower window functions by simply replacing the spherical harmonic coefficients in equation (62) by expansion coefficients using a different set of functions, obtained by solving a certain eigenvalue problem. If it is found that for a 20° galactic cut, the window functions widths can be brought down to $\Delta\ell \sim 1$ for all ℓ , corresponding to a relative smearing of less than a percent at $\ell \sim 200$, the scale of the first CDM Doppler peak. In other words, as long as none of the models between which we are trying to discriminate have any sharp spectral features causing the power spectrum to jump discontinuously from one multipole to the next, then virtually no information at all is lost in our quadratic compression.

In general, smoothing only destroys information if there are features on the smoothing scale or below it. If the true power spectrum is similar to a CDM spectrum, it will typically vary on scales $\Delta\ell \sim C_\ell/(dC_\ell/d\ell) \sim 100$, at least for angular scales $\ell \gtrsim 50$. In other words, even smoothing it with window functions with $\Delta\ell$ as large as 10 would hardly destroy any information at all about this part of the power spectrum. The quadratic compression of T96 produces a spectral resolution of $\Delta\ell \sim 1/\theta$, where θ is the smallest dimension of the patch of sky analyzed, in radians. In other words, we can allow ourselves even more leeway than the galaxy cut dictates without losing information. This can be used to save CPU-time in practice. Since we can achieve the spectral resolution $\Delta\ell \sim 10$ with $6^\circ \times 6^\circ$ patches of sky, we can form compressed data sets \mathbf{y} separately for a mosaic of such patches covering all the available sky, thus radically reducing the size of the matrices that we need to diagonalize for the T96-method, and then simply average these different estimates of the power spectrum.

5.3.2 The final squeeze: KL-method

Although the above-mentioned prescription will reduce the size of the data set dramatically, from perhaps 10^7 numbers to about 3000, there will still be considerable amounts of redundancy, since power spectrum estimates y_ℓ for neighboring ℓ -values will be correlated. Because of this, it is worthwhile to subject the new data set \mathbf{y} to a regular KL-compression. We thus term the above-mentioned quadratic step *pre-compression*: it does by no means need to be optimal, and is simply done to reduce the data set down to a small enough size that it can be fed into the KL-machinery without practical difficulties.

The values y_ℓ are Gaussian to an excellent approximation for $\ell \gtrsim 50$, by the central limit theorem, since they are the sum of $2\ell+1 \gtrsim 100$ independent numbers. The remainder, however, are not. Since the Gaussian property makes such a dramatic simplification both in the compression step and in the likelihood analysis itself, we therefore recommend discarding the y_ℓ -values with $\ell < 50$ and replacing them by the 2500 spherical harmonic coefficients $a_{\ell m}$ with $\ell < 50$ before proceeding to the KL-compression step. This way, the entire data set \mathbf{y} will be Gaussian. In addition, no information whatsoever has been lost about the largest angular

scales, where some models in fact do predict rather sharp spectral features which could render the quadratic compression step inappropriate.

In summary, we argue that the following prescription for analyzing future 10^7 pixel CMB map will be fairly close to optimal:

(i) Foregrounds are subtracted making maximal use of multifrequency data and spatial templates obtained from other experiments.

(ii) The most contaminated regions, for instance the galactic plane, are discarded altogether.

(iii) The remaining sky is expanded in spherical harmonics up to $\ell = 50$ and the coefficients saved.

(iv) This remaining sky is covered by a mosaic of overlapping regions, whose diameter are of order $5^\circ - 10^\circ$.

(v) The angular power spectrum is estimated separately from each of these patches with the method of T96, up to $\ell = 3000$.

(vi) All these power spectrum estimates are averaged.

(vii) The first 50 multipole estimates are discarded, and replaced by the 2500 numbers from step (iii).

(viii) The resulting data set (about 5500 numbers) is compressed with the KL-method.

(ix) All cosmological parameters of interest are estimated jointly from this compressed data set with a likelihood analysis.

5.3.3 Open problems

The above prescription for quadratic compression was necessarily rather sketchy, since a detailed treatment of these issues would go well beyond the scope of this paper. Indeed, the discussion above left several important questions unanswered, which are clearly worthwhile topics for further research. Here are two such examples:

- How can information loss during pre-compression be minimized? Above we merely showed pre-compression to be lossless in the absence of noise (or with identical noise levels in all pixels). In the presence of noise, one would expect lossless compression to involve some form of inverse-variance pixel weighting, *i.e.*, giving less weight to noisier pixels. On the other hand, pushing such noise weighting too far could broaden the window functions to the point where low spectral resolution led to irreversible information loss.

- How is quadratic pre-compression best implemented numerically? For instance, are there particularly choices of shapes and sizes of the above-mentioned patches that substantially facilitate the calculation of the final mean vector and correlation matrix? Is a direct analytic calculation of these quantities feasible (\mathcal{C} involves terms quadratic in the power spectrum), or is it faster to resort to Monte Carlo techniques for this step?

5.4 Real-world galaxy surveys

Also for large future galaxy surveys, some form of pre-compression appears to be necessary before a KL-compression can be done. If we wish to retain all the information on clustering down to say $3h^{-1}$ Mpc scales in a 3D volume of typical dimension $300h^{-1}$ Mpc, we clearly need to “pixelize” it into

at least $(300/3)^3 = 10^6$ numbers. Since even the power spectrum in the deeply non-linear regime contains valuable cosmological information, it would not seem justified to simply ignore these small scales.

Unfortunately, the galaxy survey problem is considerably more difficult than the corresponding CMB problem in that information about, for instance, redshift space distortions lies hidden not merely in the overall power spectrum, but also in the phases, in the differences between radial and transverse clustering patterns.

As we have noted, transforming to weighted harmonic amplitudes is one way of reducing the number of data “points” without losing cosmological information. For instance, in the case of the analysis of the 1.2Jy survey by HT95 and BHT95, only the first 1208 modes were used from the 2000 galaxies, with the limit on modes used being set by the survey size and the smallest scale still in the linear regime. However, if the full range of available modes is desired, we might need higher order compression options.

One way to implement quadratic compression, while retaining the important phase information, is to transform to some coordinate basis which is orthogonal in redshift-space. We can then apply the quadratic compression to estimate a “power spectrum” in the transformed space, having lost none of the underlying phase information. Some progress along the lines of finding an orthonormal basis function for redshift space has been made by Hamilton & Culhane (1995). However, these methods still fail to adequately deal with shot-noise and the phase mixing introduced by a finite angular mask function.

Thus the issue of whether one can do even better with galaxy surveys, while staying within the realms of numerical feasibility, remains a challenging open question.

6 CONCLUSIONS

We have given a comprehensive discussion of how to best estimate a set of cosmological parameters from a large data set, and concluded the following:

- Well-known information-theoretical results roughly speaking state that a brute-force likelihood analysis using the entire data set gives the most accurate parameter determination possible.

- For computational reasons, this will be unfeasible for the next generation of CMB maps and galaxy surveys.

- The solution is to use a good data compression scheme.

- The optimal *linear* compression method is the Karhunen-Loève method, of which the so-called signal-to-noise eigenmode method is a special case.

- Although the standard KL-method applies only when estimating a single parameter, it can be generalized to the multi-parameter case by simply adding a step consisting of a singular value decomposition (SVD).

- This SVD step also provides a simple way out of the Catch-22 situation that one needs to specify the parameter values before one has measured them.

- The KL-method produces a compression factor ~ 10 for typically sampled CMB maps, and also for the redshift space distortion analysis of Heavens & Taylor (1995).

- However, this is not enough to handle a high-resolution next generation CMB map.

• Fortunately, it appears as though this can be remedied by adding a quadratic pre-compression step without substantial information loss.

Cosmology, which used to be a data-starved science, is now experiencing a formidable explosion of data in the form of both CMB maps and galaxy redshift surveys. Around the turn of the millennium, we will probably be equipped with data sets so rich in information that most of the classical cosmological parameters can — in principle — be determined with accuracies of a few percent or better. Whether this accuracy will be attainable also in practice depends crucially on what data-analysis methods are available. We have argued that the prospects of achieving this accuracy goal are quite promising, especially on the CMB side (which is slightly simpler), by using a multi-parameter generalization of the Karhunen-Loève method together with a quadratic pre-compression scheme. However, much work remains to be done on precompression issues to ensure that we can take full advantage of the wealth of data that awaits us.

ACKNOWLEDGMENTS

The authors wish to thank Ted Bunn, Andrew Hamilton and our referee, Uros Seljak, for useful comments and suggestions. This work was supported by a PPARC research assistantship (to ANT), European Union contract CHRX-CT93-0120, Deutsche Forschungsgemeinschaft grant SFB-375 and NASA through a Hubble Fellowship, #HF-01084.01-96A, awarded by the Space Telescope Science Institute, which is operated by AURA, Inc. under NASA contract NAS5-26555.

REFERENCES

- Bennett, C. L. *et al.* 1996, ApJ, 464, L1
 Bond, J. R. *et al.* 1994, Phys. Rev. Lett., 72, 13
 Bond, J. R., 1995, Phys. Rev. Lett., 74, 4369
 Bunn, E. F. 1995, Ph.D. Thesis, U.C. Berkeley, *ftp pac2.berkeley.edu/pub/bunn*
 Bunn, E. F., Sugiyama N. 1995, ApJ, 446, 49
 Bunn, E. F., Scott, D. & White, M. 1995, ApJ, 441, L9
 Davis M., Peebles P. J. E., 1983, APJ, 267, 465
 Dodelson, S., Gates, E. & Stebbins, A. 1996, ApJ, 467, 10
 Feldman H. A., Kaiser N., Peacock J. A., 1994, APJ, 426, 23
 Fisher, R. A. 1935, J. Roy. Stat. Soc., 98, 39
 Fisher K. B., Huchra J. P., Strauss M. A., Davis M., Yahil A., Schlegel D., 1995, ApJS, 100, 69
 Górski, K. M. 1994, ApJ, 430, L85
 Gunn, J., Weinberg, D., 1995, in *Wide-field spectroscopy and the distant universe*, proc. 35th Herstmonceux conference, eds S.J. Maddox & A. Aragón-Salamanca, World Scientific, p3
 Hamilton, A. J. S, Culhane, M., MNRAS, 278, 73
 Heavens, A. F., Taylor, A. N., 1995, MNRAS, 483, 497
 Hu, W. & Bunn, E. F. & Sugiyama, N. 1995, ApJ, 447, L59
 Hu, W., Scott, D., Sugiyama, N. & White, M. 1995, Phys. Rev. D, 52, 5498
 Jungman, G., Kamionkowski, M., Kosowsky, A. & Spergel, D. N. 1996a, Phys. Rev. Lett., 76, 1007
 Jungman, G., Kamionkowski, M., Kosowsky A. & Spergel D. N. 1996b, Phys. Rev. D, 54, 1332
 Kaiser, N. 1987, MNRAS, 227, 1
 Karhunen, K., *Über lineare Methoden in der Wahrscheinlichkeitsrechnung* (Kirjapaino oy. sana, Helsinki, 1947).
 Kendall M. G., Stuart, A., 1969. *The Advanced Theory of Statistics*, Volume II, Griffin, London
 Kenney, J. F. & Keeping, E. S. 1951, *Mathematics of Statistics, Part II*, 2nd ed. (Van Nostrand, New York).
 Knox, L. 1995, Phys. Rev. D, 52, 4307
 Lawrence, A., Rowan-Robinson, M., Saunders, W., Parry, I., Xia Xiaoyang, Ellis R. S., Frenk, C.S., Efstathiou, G. P., Kaiser, N., Crawford, J., 1996, to be submitted to MNRAS
 Liddle, A. R. *et al.* 1996, MNRAS, 281, 531
 Peacock, J. A. & Dodds 1994, MNRAS, 267, 1020
 Press, W. H., Teukolsky, S. A., Vetterling, W. T., Flannery, B. P., 1992, *Numerical Recipes*. Cambridge University Press, Cambridge
 Saunders, W. *et al.* 1996, in preparation
 Scott, D., Srednicki, M. & White, M. 1994, ApJ, 421, L5
 Seljak, U. & Bertschinger, E. 1993, ApJ, 417, L9
 Seljak, U. & Zaldarriaga, M. 1996, preprint astro-ph/9603033
 Smoot, G. F. *et al.* 1992, ApJ, 396, L1
 Taylor, K., 1995, in *Wide-field spectroscopy and the distant universe*, proc. 35th Herstmonceux conference, eds S.J. Maddox & A. Aragón-Salamanca, World Scientific, p15
 Tegmark, M., Bunn, E. F. 1995, ApJ, 455, 1
 Tegmark, M. 1995, ApJ, 455, 429
 Tegmark, M. 1996, MNRAS, 280, 299
 Tegmark, M. & Efstathiou, G. 1996, MNRAS, 281, 1297
 Therrien, C. W. 1992, *Discrete Random Signals and Statistical Signal Processing* (Englewood Cliffs: Prentice Hall)
 Vogeley, M. S. 1995, in “Wide-Field Spectroscopy and the Distant Universe”, eds. Maddox & Aragón-Salamanca (World Scientific, Singapore)
 Vogeley, M. S. & Szalay, A. S., 1996, ApJ, 465, 34
 White, M. & Bunn, E. F. 1995, ApJ, 450, 477
 Yamamoto, K. & Bunn, E. F. 1996, ApJ, 464, 8